On the activity – or lack thereof – of RuO_2 based electrodes in the electrocatalytic reduction of CO_2

Stefano Mezzavilla [§,†,*], *Yu Katayama* [⊿,ǁ], *Reshma Rao* [#], *Jonathan Hwang* [‡], *Anna Regoutz,* [ǀ] *Yang Shao-Horn* [⊿,#,‡], *Ib Chorkendorff* [§], *Ifan E.L. Stephens* [§,ǁ,*]

§ SurfCat, Department of Physics, Technical University of Denmark, DK-2800 Kgs. Lyngby, Denmark

ǁ Department of Materials, Imperial College London, Royal School of Mines London SW72AZ, England

⊿ Research Laboratory of Electronics, ‡Department of Materials Science and Engineering, # Department of Mechanical Engineering, Massachusetts Institute of Technology, Cambridge, MA 02139, USA

‖ Department of Applied Chemistry, Graduate School of Sciences and Technology for Innovation, Yamaguchi University, Tokiwadai, Ube, 755-8611, Japan

† Current Address: Department of Materials, Imperial College London, Royal School of Mines London SW72AZ, England

KEYWORDS

CO_2 electrocatalytic reduction • Ruthenium dioxide • in situ spectroscopy • methanol

ABSTRACT

RuO_2-based electrodes have been extensively studied for several electrochemical reactions. Earlier literature works claim RuO_2-based catalysts to be active also for the electrocatalytic conversion of CO_2 to methanol with high selectivity at very low overpotentials. Here we report a thorough investigation of RuO_2 films and particles for the electrocatalytic reduction of CO_2. The different experimental configurations explored in our work showed that H_2 is basically the only reaction product under CO_2 reduction conditions in contrast to earlier reports. In situ surface enhanced infrared absorption spectroscopy (SEIRAS) measurements revealed that CO bound to the RuO_2 surface, albeit acting solely as spectator species. Our experiments indicated that adsorbed CO cannot be reduced further to methanol or other CO_2 reduction products.

INTRODUCTION

The electrocatalytic reduction of CO_2 is a promising strategy to synthesize commodity chemicals and fuels exploiting renewable energy resources. Major breakthroughs are necessary to discover efficient catalysts capable to maximize the production of high-value products.[1–3] Copper is the most efficient known, monometallic catalyst capable to reduce CO_2 and CO to multi-carbon hydrocarbons and oxygenates like ethylene and ethanol.[4–6] The electrochemical synthesis of methanol from CO_2 is more difficult and, to the best our knowledge, with monometallic catalysts, this product has been observed only in minute amounts at high overpotentials.[7] While the activity of mono and (bi)metallic transition metals have been largely mapped out,[4,8] stable conductive oxides remain largely unexplored catalysts.

RuOx-based materials have been extensively studied as electrodes for supercapacitors[9] and as catalysts for the hydrogen evolution reaction,[10] chlorine evolution reaction[11] and oxygen evolution

reaction.[12] Several earlier literature works claim RuO_2-based oxides to be active catalysts for the electrocatalytic reduction of CO_2 to methanol with high selectivity at very low overpotentials. To our knowledge, Bandi and co-workers are the first to explore this class of materials. They studied binary RuO_2/TiO_2 and multi-components $RuO_2/TiO_2/SnO_2/MoO_2$ mixtures reporting Faradaic efficiency for CH_3OH up to 24 % at ~ -0.15 V_{RHE} in 0.05 M H_2SO_4 (pH 1.2). They reported a Faradaic efficiency of 74 % by operating the RuO_2/TiO_2 catalysts in a phosphate buffer (pH 4) at an undefined potential labelled as "near water reduction potential".[13,14] They found that the performance of RuO_2/TiO_2 mixed oxides can be further improved by adding Cu species on the surface (up to ~30% Faradaic efficiency for a Cu-doped 75:25 Ru:Ti electrode).[14] Faradaic efficiency towards CH_3OH up to 30% at -0.15 V_{RHE} were reported also with Cd and Cu modified RuO_2 electrodes in 0.5 M $KHCO_3$.[15] Qu et al. studied RuO_2 particles supported on TiO_2 nanotubes and registered a selectivity towards CH_3OH up to 60% at -0.15 V_{RHE}.[16] By comparing the performance of RuO_2 particles deposited on boron-doped diamond and TiO2 substrates, Spataru et al. later postulated that the interaction between RuO_2 and the TiO_2 substrate is instrumental to achieve high yield of CH_3OH.[16] More recently, Ullah et al. investigated $Ir_{0.8}Ru_{0.2}$ films and reported the formation of a variety of oxygenates at -0.7 V_{RHE} in an organic buffer solution.[17] Ab initio calculations have rationalized the aforementioned experimental findings by identifying possible reaction paths for the production of CH_3OH and $CHOO^-$ with RuO_2, deped-RuO_2 and Ru-Ir catalysts.[18–21]

Motivated by the preliminary studies presented above, we aimed at inspecting this class of materials for the electrocatalytic CO_2 reduction more in depth. The interest towards RuO_2 and other oxides is well motivated by their rich chemistry, which offers plenty of scope to tune their textural and electronic surface features.[22–24] Indeed, this flexibility is potentially a strong asset for

tuning their electrocatalytic behavior, thus maximizing the production of desired compounds. Here we report a thorough investigation of RuO_2 films and particles for the electrocatalytic reduction of RuO_2. The electrochemical performance of this class of materials was thoroughly assessed, with particular attention to the formation of methanol or other oxygenates. We discuss the stark contrast between our results and prior literature reports.

RESULTS

Electrodes Characterization. Three different forms of RuO_2 electrodes were investigated: RuO_2 films prepared via thermal decomposition of $RuCl_3$ and $Ru(NO)(NO)_3$ as well as commercial RuO_2 particles. Figure 1b shows representative scanning electron microscopy (SEM) images of RuO_2 films prepared via thermal decomposition of $RuCl_3$. The Ti substrate is covered by a rough nanocrystalline RuO_2 layer, which forms a homogenous film for high catalyst loadings while it fragments in patches for lower loadings. Similar structures were observed with films prepared starting from $Ru(NO)NO_3$. The commercial RuO_2 particles (Figure 1c) display an agglomerated nanocrystalline structure with primary units of ~ 50-100 nm in size. The X-ray diffraction patterns (Figure 1a) confirm the catalysts have a rutile crystalline structure and the XPS spectra agree with a typical RuO_2 core-level profile (Figure S1).

The physical and electrochemical characterization of Ti supported RuO_2 films prepared via the thermal decomposition of metal precursors has been the subject of numerous studies, particularly in relation to supercapacitors[9] and dimensionally stable anodes.[25–27] The initial electrochemical surface area was monitored via cyclic voltammetry (CV) in CO_2 saturated 0.1 M $KHCO_3$ (Figure S2 and S3 for detailed discussion). The charge derived from the integration of the CVs recorded with films and RuO_2 particles at increasing loadings is shown in Figure 2a. We note how the measured capacitance decreases with higher scan rates (Figure S 3). The concept of inner/outer

surfaces is recalled to explain this behavior.[28,29] A scan rate of 20mVs^{-1} and an average surface specific charge of 100 μFcmRuO_2^{-2} was used for the calculations in this work.[28] As expected for nanostructured electrodes having an increasing catalyst loading with fully accessible active surface area, a linear behavior is visible for RuO_2 particles.

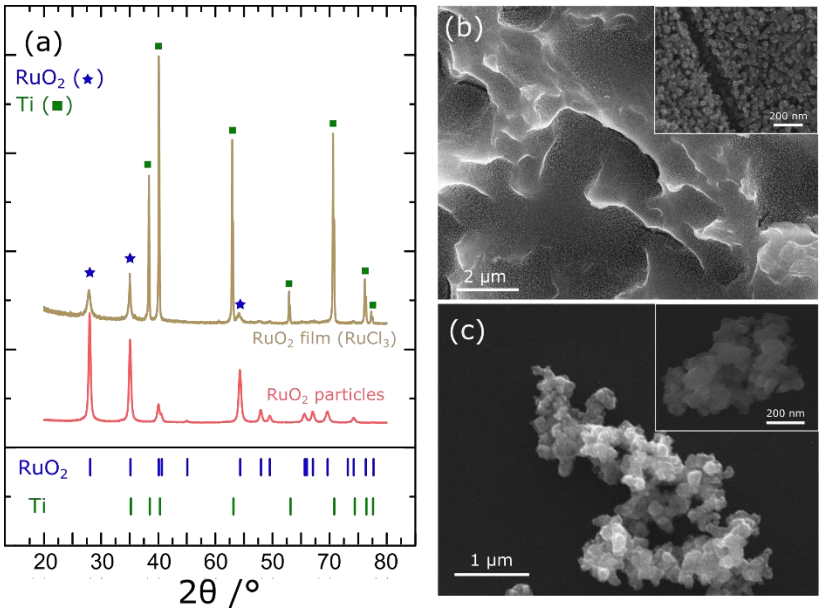

Figure 1. *(a) X-ray diffraction patterns of commercial RuO_2 particles and RuO_2 film (from $RuCl_3$) deposited on etched Ti electrode. The expected reflections for rutile RuO_2 (star symbol) and the Ti hcp (square symbol) phases are reported at the bottom of the plot and on top of the diffraction pattern for the RuO_2 film. Rutile RuO_2 Powder Diffraction File (PDF): 01-088-0285; hcp Ti PDF: 01-077-0447 41-1445. (b) and (c) Scanning Electron Microscopy images of RuO_2 film and particles, respectively. The insets report magnified details of the structures.*

In contrast, the charge measured with RuO_2 films prepared from $RuCl_3$ approaches a plateau at high loadings, indicating the formation of a thick film and resulting in a poor utilization of the catalyst. The extrapolated electrochemical active surface area (ECSA) corresponds to ca. 14 m^2g^{-1} for films with low loadings and to 2 m^2g^{-1} for thicker films (Figure 2b). For RuO_2 particles, the

measured specific surface area (~10 m^2g^{-1}) is independent of the loading. This value is in good agreement with the specific surface area measured via N_2 physisorption and with simple geometrical considerations (primary units of 50-100 nm in size). At identical loadings, the charge measured with RuO_2 films prepared from $Ru(NO)NO_3$ consistently showed higher capacitance. It is suggested that the lower decomposition temperature of $RuCl_3$ precursors leads to electrodes with a higher degree of crystallinity and, in turn, with a lower electrochemical surface area.[27]

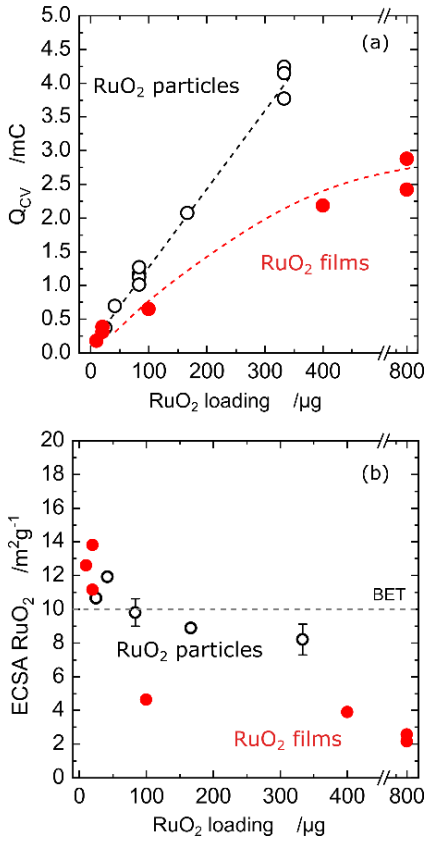

Figure 2. (a) *Charge derived from the integration of the cyclic voltammograms recorded with RuO_2 films and particles in CO_2 sat. 0.1M $KHCO_3$ (0.3-1 V_{RHE}, 20 mVs^{-1}) and varying catalyst loadings. See Figure S2 for an example of cyclic voltammogram (b) Corresponding electrochemical active surface area. An average surface specific charge of 100 $\mu FcmRuO_2^{-2}$ was used for the calculations.[28] The surface area measured for RuO_2 nanoparticles via N_2 physisorption (BET) is indicated.*

CO_2 electrolysis with RuO_2 electrodes

CO_2 electrolysis experiments were carried out with the three types of RuO_2-based catalysts, always using fresh electrodes. The tests were performed in chronoamperometric mode at potentials ranging from -0.1 V_{RHE} to -0.9 V_{RHE}. A total charge of 15 C was passed in each experiment. The accumulated reaction products were quantified by gas and liquid chromatography at the end of each experiment. Figure 3 summarizes the Faradic efficiency measured with RuO_2 electrodes prepared via thermal decomposition of $RuCl_3$.

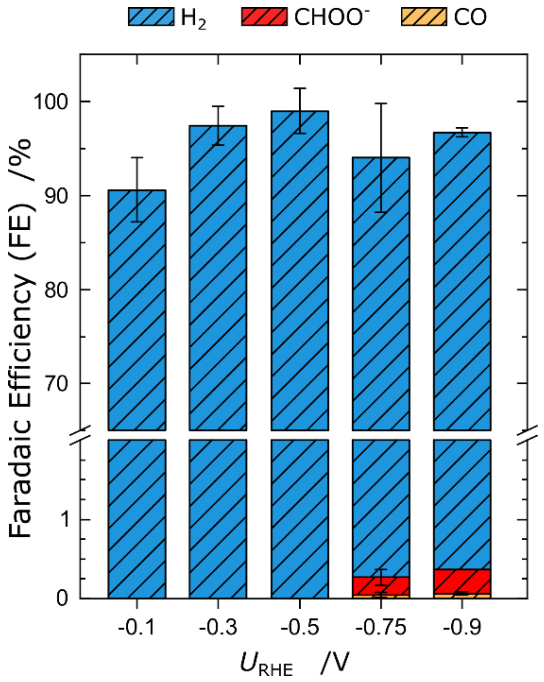

Figure 3. *Faradaic Efficiency (FE) measured during CO_2 electrolysis experiments with RuO_2 electrodes (prepared from thermal decomposition of $RuCl_3$) in CO_2 saturated 0.1 M $KHCO_3$. A total charge of 15C was passed through the electrode for each experiment. See the Experimental Methods and the Supporting Information for more details concerning the electrochemical and analytical procedures.*

At potentials more anodic than -0.75 V_{RHE}, H_2 was the only product detected. We note that the charge balance is close to 100% in all the cases: this indicates that the totality of the electrons being transferred at the electrochemical interface was accounted for. At -0.1 V_{RHE}, because of the low current densities (typically below 0.5 $mAcm^{-2}$), long chronoamperometric measurements (> 15 h) were required to transfer a total of 15 C. Consequently, a small fraction of the produced H_2 escaped the cell, causing the charge balance to drop below 95%. At potentials more cathodic than -0.75 V_{RHE} traces of CO and $CHOO^-$ (Faradaic efficiencies of ~0.05% and ~0.2%, respectively) were detected. Similar results were obtained with RuO_2 films prepared from $Ru(NO)(NO)_3$ and with commercial RuO_2 particles (Figure S4). Methanol was not detected under any conditions. We note that the presence of oxygenates or other CO_2 reduction products was carefully monitored for each experiment via head space gas chromatography and HPLC. Based on the detection limit for CH_3OH (~10 μM, Figure S5), the volume of the electrolyte (12mL) and a total charge of 15 C, we were able to detect the formation of CH_3OH down to ~0.5% in Faradaic efficiency. The contribution of the substrates (Ti/TiO_2 for RuO_2 films and glassy carbon for RuO_2 particles) is negligible compared to the current registered with the RuO_2 catalysts (Figure S6).

Surface adsorbates under CO_2 reduction conditions

In order to understand whether CO_2 and CO interact with the RuO_2 surface, a series of chronoamperometry experiments were carried out with RuO_2 films in 0.1 M $HClO_4$. The electrolyte, initially saturated with Ar, was purged with CO_2 (or CO) after 300 s while keeping the electrode under potential control (Figure 4). The use of an acidic media allowed us switching from Ar to CO_2 (or CO) saturated electrolytes without changing the pH of the electrolyte. In parallel, we performed a series of *in situ* surface enhanced infrared absorption spectroscopy (SEIRAS) measurements on a RuO_2 nanofilm sputtered on a roughened Pt surface using a similar measuring

protocol (Figure S7). When the electrolyte was saturated with Ar, the registered current is completely ascribed to the hydrogen evolution reaction (HER) and no detectable adsorbates were observed in the SEIRA spectra. Immediately after the introduction of CO (or CO_2), the total current density decreased drastically. The current drop was more pronounced with CO at mild cathodic potentials (-0.2 to -0.5 V_{RHE}), while it was less severe at -0.75 V_{RHE}. SEIRAS measurements at -0.5 V_{RHE} showed two distinct peaks at ca. 1870 cm^{-1} and ca. 1660 cm^{-1} appearing upon the introduction of CO, which correspond to linear-bound CO adsorbates[30] and interfacial water,[31] respectively.

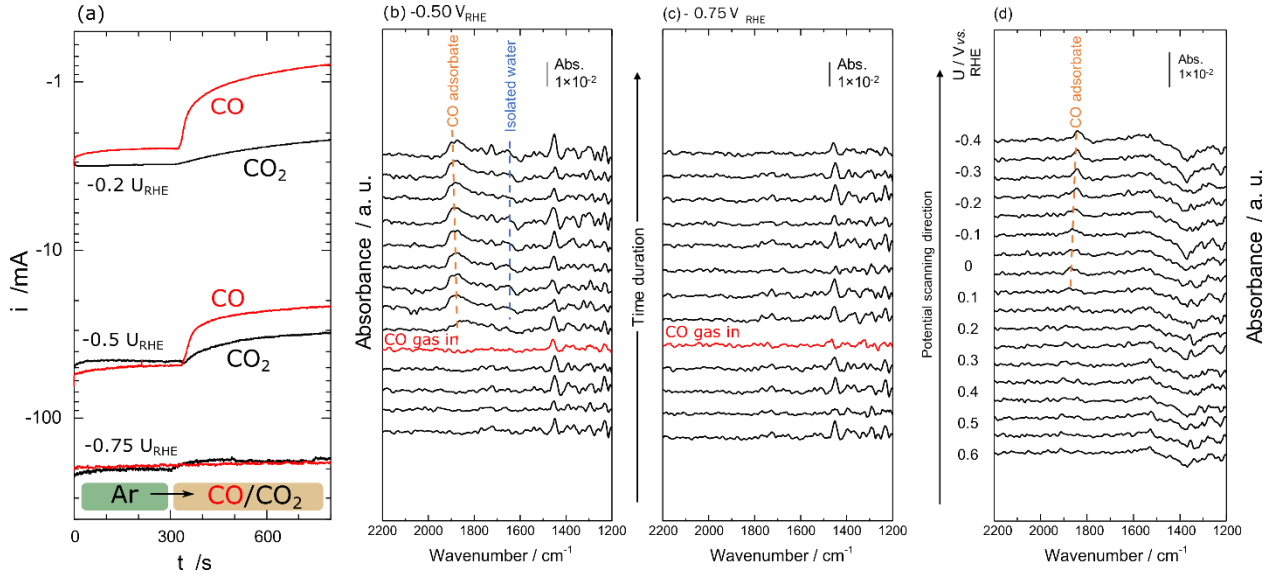

Figure 4 *Surface adsorbates under CO_2 reduction conditions. (a) CO_2/CO dosing experiments carried out in 0.1 M $HClO_4$ with a RuO_2 film prepared from $RuCl_3$ (100µg RuO_2). (b-c) Surface enhanced infrared absorption (SEIRA) spectra for a RuO_2 nanofilm deposited on a roughened Pt surface at (b) -0.5 V_{RHE}, (c) -0.75 V_{RHE} and (d) SEIRAS in CO_2 saturated 0.1M $KHCO_3$. A cathodic potential sweep was applied to the electrode while recording the spectra. The SEIRAS experiment with Ar/CO_2 in 0.1 M $HClO_4$ is reported in figure S9.*

In our previous experimental work we probed the interaction of CO with a Pt substrate in 0.1 M $HClO_4$. We observed a distinct couple of sharp peaks of CO species adsorbed in the linear (>2075 cm^{-1}) and bridged (>1850 cm^{-1}) configuration.[32] The peaks observed on Pt are distinct from the 1870 cm^{-1} peak observed in this study, confirming that the roughened Pt substrate is not responsible for the adsorbed CO signal in the current study. The relatively thick RuO2 film (ca. 30 nm) ensures the absence of indirect electronic effects between the Pt substrate and RuO2 film. No detectable peaks were observed when the same measurement was performed at more negative potentials (-0.75 V_{RHE}), suggesting a lower degree of interaction between CO and the RuO_2 surface, in agreement with the chronoamperometric test at -0.75 V_{RHE}. Furthermore, a similar CO stretching peak was detected when CO_2 was introduced at -0.5 V_{RHE}, indicating that CO_2 can be reduced to CO in an electrochemical environment (see Figure S8). The interaction of CO_2/CO with RuO_2 was also observed via SEIRAS experiments in CO_2 saturated 0.1 M $KHCO_3$ electrolyte (Figure 4d, potential is swept catholically during the scan). However, since H_2 is the only product detected under cathodic potentials, and no other peaks were registered in the SEIRAS measurement, the CO adsorbate can be considered as a spectator species that does not get further reduced.

Mixed RuO_2 oxides

Our results show that RuO_2 electrodes are inactive for the CO_2 electrocatalytic reduction, irrespective of the preparation methods and the applied potential. We further explored the catalytic performance of mixed Ru-Ti and Ru-Sn oxides to elucidate whether the presence of heteroatoms in the lattice structure is key for the formation of CH_3OH or other oxygenates. The mixed oxides were prepared by thermal decomposition of precursors mixtures, exactly reproducing the preparation used by Bandi et al. in their works.[13,14] It is established that mixed Ru-Sn oxides

monophasic solid solutions can be prepared over the whole composition range.[33] In contrast, the crystal structure of mixed Ru-Ti oxide is subject of controversy.[34,35] Several studies on Ru-Ti oxide prepared via thermal decomposition (same procedure used in our work) postulate the formation of a (meta)stable solid solution for a large compositional window.[34,36] In contrast, oxides prepared via sol-gel routes tend to result in two separate phases.[37] Our XRD results (Figure S11) showed the formation of a monophasic solid solution for Ru-Sn oxides and for Ru:Ti of 50:50 (at:at), while a biphasic structure was formed increasing the Ti content (Ru:Ti of 25:75).

Figure 5(a) shows the Faradaic efficiency measured with Ru-Ti oxides at -0.75 V_{RHE}. Overall, the behavior is comparable to that registered with pure RuO_2 electrodes. The selectivity toward CO slightly increases (up to ~ 1%), especially for the Ti rich sample. CH_3OH or other CO_2 reduction products were not detected. Noteworthy, the current densities were smaller than the ones measured with pure RuO_2 films with comparable catalyst loadings, suggesting that the introduction of Ti atoms in the RuO_2 lattice is detrimental for the HER kinetics. No evident reduction of the oxides was observed via electrochemical methods, indicating that the metastability known for RuO_2 is likely to be retained also with Ru-Ti oxides. In their report, Bandi et al.[14] observed an increase in the CH_3OH yield with Cu-decorated Ru-Ti oxides. In order to verify this possibility, we electrodeposited Cu species onto Ru:Ti electrode following the procedure described by Bandi et al.[14] The electrodeposition resulted in the formation of large Cu particles (> 200nm) physically well dispersed on the Ru-Ti surface (Figure S12). At -0.75 V_{RHE}, the as-prepared Cu-decorated electrode showed a selectivity towards of CO and $CHOO^-$ of ~11% and 5%, respectively. Hydrogen remains the most abundant product. Collectively, the electrode operated as a physical mixture of the two constituents (Cu particles and Ru-Ti oxide). Indeed, in this potential window Cu is expected to give small amounts CO and $CHOO^-$.[38] In support of this hypothesis, traces of

CH_4 (know product of CO_2 reduction with Cu catalysts) were detected when the electrode was tested at -1 V_{RHE}.

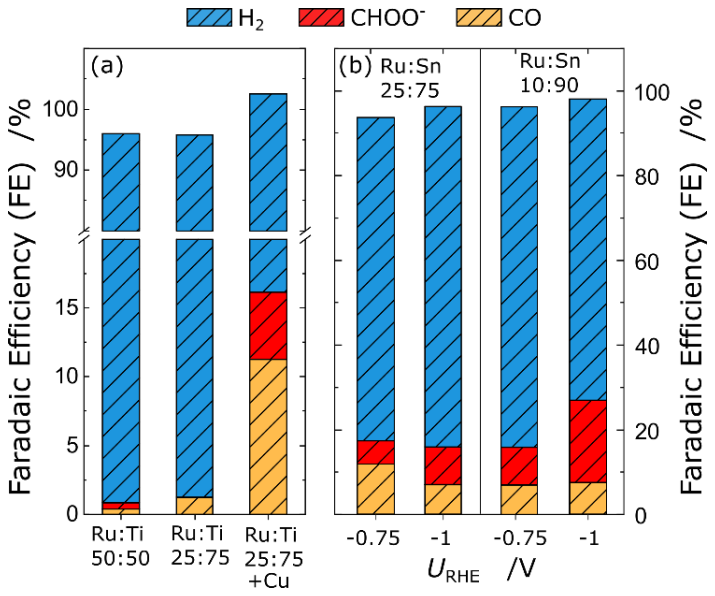

Figure 5 (a) *Faradic efficiency measured during CO_2 electrolysis experiments with Ru-Ti and Cu decorated Ru-Ti oxide films in CO_2 saturated 0.1 M $KHCO_3$ at -0.75 V_{RHE}. (b) Faradaic efficiency measured with Ru-Sn oxide films at different potentials in CO_2 saturated 0.1 M $KHCO_3$. See the Experimental Methods and the Supporting Information for more details concerning the electrochemical and analytical procedures.*

Figure 5b shows the Faradaic efficiency measured with Ru-Sn oxides (Ru:Sn atomic ratio of 25:75 and 10:90) at -0.75 V_{RHE} and -1 V_{RHE}. Sn-rich oxides display a distinct behavior from the Ru:Ti electrodes. Even though H_2 remains the most abundant product and CH_3OH was not formed at any potential, appreciable amounts of CO and $CHOO^-$ were detected. With a Ru:Sn (10:90) composition, the total selectivity towards CO_2 reduction products reached ~ 25% at -1 V_{RHE}. At this point, we cannot ascertain the chemical state of the surface under reaction conditions. We cannot exclude a (partial) reduction involving the surface layers and/or the bulk of the oxide,

consistent with reports by others on pure SnO_2 catalysts.[39,40] Overall, besides a purely scientific interest, Ru-Sn oxides do not seem to be promising catalysts for CO_2 reduction.

DISCUSSION

The evidence presented in the previous sections clearly shows that RuO_2 and mixed RuO_2 catalysts are not active for the conversion of CO_2 to methanol, which is in stark contrast with what highlighted in past literature. While reviewing previous works, we carefully examined the experimental procedures sifting for the decisive detail in the preparation of the electrodes or for the critical measuring conditions. We first hypothesized that the nature of the RuO_2 precursor (i.e. $RuCl_3$ or $RuNO(NO)_3$) could have been a decisive factor. However, the concurrent results obtained with different precursors and commercial catalysts clearly indicated that this variable affects the physical features of the catalysts, but not their electrochemical behavior. In addition, this argument rules out the possibility that residual Cl species (from decomposition of $RuCl_3$) might influence the catalytic events. The impact of the reaction temperature was briefly explored (results not shown). Some of the past works were carried out at temperature below 5°C.[17,41] At 4°C, we did not observe the formation of CO_2 reduction products and H_2 remained the only gas evolved. Under these conditions we only observed changes in hydrogen evolution current densities, readily explained by intrinsically slower kinetics. We note that it is impossible to pinpoint the reason behind the discrepancy between our findings and past literature data: such a task would go beyond the scope of this manuscript. Moreover, we cannot exclude the notion that RuOx-containing catalysts could be engineered to yield a more favorable performance for CO_2 electroreduction. Nonetheless, it is important to provide some considerations relative to the controversial results reported for RuO_2 electrodes. In hindsight, on a qualitative basis, the reported formation of CH_3OH

at potential as low as -0.150 V_{RHE} is challenging to rationalize, especially considering that the thermodynamic potential for CO_2 protonation to CH_3OH is ~ 0 V_{RHE} and an overpotential above 1.0 V is required to produce traces amounts of CH_3OH with pure metal catalysts.[7] The research effort put in place over the last decade has produced a solid code of practice for experimental work on the electrocatalytic conversion of CO_2, especially with respect to fundamental research. Several recent manuscripts have highlighted a comprehensive set of testing and analytical aspects that one must consider to avoid experimental artefacts caused by ill-defined experimental conditions, deficient analytical protocols or by the presence of adventitious (metallic) impurities.[42–44] Many of the preliminary papers reporting the formation of CH_3OH used poorly defined experimental procedures and insufficient analytical methods. Popic et al, for instance relied entirely on infrared spectroscopy and cyclic voltammetry for the detection of reaction products.[13] In addition, the description of the experimental methods often lacks details (e.g., applied potential defined as "near water reduction potential").[13,14] Moreover, a number of works highlighted in the introduction employed buffers containing organic species (i.e., acetic acid for Britton–Robinson buffer solutions) as electrolytes.[17,41] The presence of organic species may introduce a number of artefacts. In all the past investigations the amount of evolved H_2 was never quantified. The quantification of this by-product is important not only for completeness sake, but also to ensure that the overall charge balance is met, and all the reaction products are accounted for.[4]

Although we could not detect the formation of CH_3OH under any circumstance, the electrochemical and SEIRAS results presented in Figure 4 clearly show that CO and CO_2 do bind to the RuO_2 surface, thus affecting the HER kinetics. The adsorption configurations of CO on RuO_2 in the gas phase have been studied over a wide temperature range and the main findings have been summarized by Over.[22] To the best of our knowledge, the interaction between CO and RuO_2

in an electrochemical environment has been investigated only at anodic potentials (electrochemical oxidation of CO).[45,46] Our SEIRAS measurements confirm the presence of CO adsorbates (bands at ca. 1870 cm^{-1}) also at cathodic potentials. This hypothesis is supported by the existence of the H-O stretching vibration (ca. 3600 cm^{-1}, see Figure S8) and H-O-H bending vibration (ca. 1660 cm^{-1}). These vibrations may be attributed to the isolated water at the interface formed because of the hydrophobic CO adsorbates.[47] Prior vibrational spectroscopy studies suggest the coexistence of a number of adsorption and stretching configurations when a RuO_2 (110) surface is exposed to CO in the gas phase. Three different categories are identified: frequencies between 1850 and 1980 cm^{-1} and between 1980 and 2100 cm^{-1} are assigned to CO species binding to the Ru *bridge* site through a symmetric and linear (asymmetric) configuration, respectively. Frequencies between 2100 and 2155 cm^{-1} are associated to CO species binding to the Ru *cus* site in on-top configuration.[30] Based on the absence of peaks in the 2100-2155 cm^{-1} region (Figure 4), the latter case (CO adsorbed at Ru *cus* site) can be excluded: we thus infer that under the electrochemical conditions used in our work CO is likely to adsorb on the Ru *bridge* site.

An atomic-scale elucidation of the impact of CO adsorbates on the HER kinetics would require a detailed analysis that goes beyond the scope of this work. The complexity arises because (i) the exact chemical state of the surface under reaction conditions remains elusive and (ii) the HER mechanisms on RuO_2 surfaces is not yet fully understood. Experimental evidence and theoretical calculations have demonstrated that RuO_2 is partially reduced (i.e. protonated to oxyhydroxide) under cathodic conditions,[22,48–50] albeit the exact chemical state of the surface under reaction conditions remains experimentally undetermined. The extend and degree of crystallinity of the hydrated phase is still matter of debate, as suggested by the different observations reported by *in situ* X-ray diffraction/reflectivity[51] and XPS studies.[48,52] Various plausible scenarios have also

been predicted by theoretical simulations.[53] Overall, the heterogeneity of these findings suggests that the chemical and crystalline state of the RuO_2 films under cathodic conditions might depend on subtle experimental variables, such as the procedure used to synthesize the electrodes. The cyclic voltammetry curves we measured after CO_2 reduction (see Figure S13) suggest a partially irreversible hydration of the RuO_2 films (see discussion in the supplementary information). We did not observe evident electrochemical features of a metallic Ru over-layer. The absorption of H^+ species within the RuO_2 structure (defined as "catalyst activation") has been observed in other studies.[52,54]

With respect to HER mechanistic aspects, a series of works published across the 1990s postulate that on a partially reduced RuO(OH) surface the HER occurs through a Volmer-Heyrovsky rate determining step involving the hydroxyl group in oxygen *bridge* site.[22,55] In contrast, a direct Ru-H (hydride) mechanism limited by a homolytic reaction (i.e., Tafel mechanism) has been recently proposed by Pastor et al. through a spectro-electrochemical analysis.[56] On a theoretical basis, the hydride mechanism could occur either at Ru *cus* site or at Ru *bridge* site (via the complete reduction of the Ru-OH group). In view of these considerations, one can hypothesize that the presence of CO/CO_2 bound on the surface negatively affects the HER performance via (i) a direct site-blocking mechanism, most likely to occur on the Ru *bridge* site since we do not have SEIRAS evidence for CO adsorbed at Ru cus site, and/or (ii) via indirect electronic mechanism, where the CO bound at the *bridge* site affects the binding energy of H^+/H_2O at the adjacent Ru *cus* site. A more detailed investigation, ideally coupled with a computational analysis, should be undertaken to shed light onto these open questions.

It is established that transition metals that bind CO (and/or CO_2) too strongly, such as Pt, Fe and Ni,[4,7,57] are very selective for the HER and inactive for CO_2 reduction. Consequently, at first sight

one could interpret the lack of CO_2 reduction activity and the detrimental impact of CO adsorbates for the HER kinetics as elements that affiliate RuO_2 electrodes to strongly CO-binding surfaces such as Pt or Fe. However, one should note that the latter are capable to give minor amounts of CH_4 and CH_3OH,[7,58] despite generally displaying high surface CO coverages under CO_2 reduction conditions.[32,59,60] In contrast, even though RuO_2 catalysts experience similar CO surface poisoning effects, they are unable to reduce CO further.

CONCLUSIONS

Several past literature reports postulate that RuO_2 catalysts are capable to electrochemically convert CO_2 to methanol with excellent selectivity at low overpotentials. We could not verify these results. All the catalysts tested, and the numerous experimental configurations explored in our work confirmed that H_2 is basically the only product detected under CO_2 reduction conditions. A series of combined electrochemical and SEIRAS experiments showed that CO and CO_2 bind to the RuO_2 surface. However, bound CO acts as spectator species and cannot be converted to methanol or other oxygenates.

EXPERIMENTAL METHODS

Electrodes Preparation

RuO_2 films were prepared by thermal decomposition of metal precursors ($Ru(NO)NO_3$ and $RuCl_3$) drop-casted onto etched Ti substrates. Ru-Ti and Ru-Sn mixed oxides were prepared starting from $RuCl_3$, $TiCl_4$ (attention, compounds reacts violently with water) and $SnCl_2$ solutions (0.15 M, 0.15 M and 0.5 M, respectively) using isopropanol as solvent. Once dried (room temperature), the electrodes were calcined at 450 °C (30 min at 90 °C, 3 °Cmin^{-1} ramp to 450 °C, 1 h dwell time) in a tubular furnace under static air. Copper-doped Ru-Ti oxides were prepared following the procedure electrodeposition procedure reported by Bandi et al.[14] RuO_2 particles

(99.9% trace metals basis) were purchased from Sigma Aldrich and used as received. More information about the electrodes preparation can be found in the Supporting Information.

Electrochemical Measurements

CO_2 electrolysis experiments were carried out in a custom-made three electrode glass H-cell. The working electrode (WE) and CE compartments were separated by a Nafion® 117 proton conducting membrane. A gold mesh (GoodFellow 99.9%) was used as counter electrode (CE). The volume of the electrolyte in the WE compartment was 12 mL. The working electrode potential (E_{WE}) was referenced against a $Hg/HgSO_4$/sat. K_2SO_4 reference electrode (SI analytics) and converted to the reversible hydrogen (RHE) scale according to:

$$E_{RHE}\ (V) = E_{WE} + E_{MSE} + 0.059 * pH$$

Where E_{WE} and E_{MSE} are the set potential at the WE (vs. $Hg/HgSO_4$/sat. K_2SO_4) and the reference electrode potential (typically 0.664 V ± 5mV vs. E_{SHE}), respectively. The reference electrode potential (E_{MSE}) was regularly checked by measuring the equilibrium potential against a $Pt|H_2$(1 atm)$|H^+$(0.1 M) electrode in 0.1 M $HClO_4$. Electrochemical measurements were conducted using a BioLogic VMP2 potentiostat controlled through the EC -Lab software. CO_2 electrolysis experiments were carried out potentiostatically (chronoamperometry) in a CO_2 saturated 0.1 M $KHCO_3$ solution (pH 6.8), prepared by bubbling CO_2 in a 0.1 M KOH aqueous solution (Merk, Potassium hydroxide hydrate 99.995 Suprapur®, solid pellets). The Ohmic resistance (R_Ω) was measured via electrochemical impedance spectroscopy (EIS) and the iR Ohmic drop was compensated for via positive feedback. The pressure in the working electrode (WE) compartment was kept at 1.1 bar. More details about the electrochemical characterization are reported in the Supplementary Information.

Products analysis

Gaseous reaction products were detected and quantified via in-line gas chromatography (GC). Liquid products were detected and quantified via head-space gas chromatography (HS-GC) and via high performance liquid chromatography (HPLC). External standards were used for the calibration of the HS-GC and HPLC analyses. Full details about the GC, HS-GC and HPLC analyses are given in the Supplementary Information.

CO and CO_2 dosing experiments

CO and CO_2 dosing experiments were conducted in a one-compartment three-electrodes glass cell equipped with a Lugging capillary connected to a $Hg/HgSO_4$/sat. K_2SO4 reference electrode. A gold mesh was used as counter electrode. Prior to each measurement, the Ohmic drop was

determined via EIS and compensated for via positive feedback. A 0.1 M $HClO_4$ (Merck Suprapur 70%) electrolyte was used for the experiments. The electrode (RuO_2 film prepared using $RuCl_3$) was held at constant potential (-0.2 V_{RHE}, -0.5 V_{RHE} and -0.75 V_{RHE}) while monitoring the current.

Surface enhanced infrared absorption spectroscopy (SEIRAS) experiments

For the *in situ* SEIRA measurements, we used a Pt working electrode composed of a thin (*ca.* 50 nm) Pt film deposited on the Si prism (radius 22 mm, Pier optics) via an electroless deposition method.[61] Magnetron sputtering was used to deposit the RuO_2 electrocatalysts. The film was sputtered on the electroless deposited Pt layer at a deposition rate of ~0.7 A/s under Ar:O_2=7:5 sccm, total pressure 3 mTorr, at 450°C, result in a thickness of ca. 30 nm, as measured by an electrochemical quartz crystal microbalance. The SEIRA spectra were recorded using a single reflection ATR accessory (Pike Vee-Max II, Pike Technologies) with the Si prism at an incident angle of 68 degrees. Before every experiment, Ar was bubbled through the electrolyte for 15 minutes in order to remove air from the solution. The prism surface was then cleaned by cycling the potential between 0.05 and 0.90 V *vs.* RHE. Details of *in situ* SEIRAS measuring procedure were described elsewhere[62,63] and in the Supplementary Information.

ACKNOWLEDGMENTS

This project has received funding from the European Union's Horizon 2020 research programme under the Marie Skłodowska-Curie grant agreement No. 705230. The support from the VILLUM Center for Science of Sustainable Fuels and Chemicals funded by the VILLUM Fonden research grant (9455) is also acknowledged. The author would like to thank Dr. A. Bhowmik, Dr. H. A. Hansen and Dr. T. Vegge (DTU Energy) for the fruitful discussions on the project.

AUTHOR INFORMATION

Corresponding Author

* Ifan E.L. Stephens (i.stephens@imperial.ac.uk)
Stefano Mezzavilla (s.mezzavilla@imperial.ac.uk)

Department of Materials, Imperial College London, Royal School of Mines London SW72AZ, England

Present Addresses

† Department of Materials, Imperial College London, Royal School of Mines London SW72AZ, England

Author Contributions

The manuscript was written through contributions of all authors. All authors have given approval to the final version of the manuscript.

Funding Sources

- European Union's Horizon 2020, Marie Skłodowska-Curie grant agreement No. 705230.
- VILLUM Fonden research grant (9455)

REFERENCES

(1) Martín, A. J.; Larrazábal, G. O.; Pérez-Ramírez, J. Towards Sustainable Fuels and Chemicals through the Electrochemical Reduction of CO_2: Lessons from Water Electrolysis. *Green Chemistry* **2015**, *17* (12), 5114–5130. https://doi.org/10.1039/C5GC01893E.

(2) Zhao, S.; Jin, R.; Jin, R. Opportunities and Challenges in CO_2 Reduction by Gold- and Silver-Based Electrocatalysts: From Bulk Metals to Nanoparticles and Atomically Precise Nanoclusters. *ACS Energy Letters* **2018**, *3* (2), 452–462. https://doi.org/10.1021/acsenergylett.7b01104.

(3) Qiao, J.; Liu, Y.; Hong, F.; Zhang, J. A Review of Catalysts for the Electroreduction of Carbon Dioxide to Produce Low-Carbon Fuels. *Chem. Soc. Rev.* **2014**, *43* (2), 631–675. https://doi.org/10.1039/C3CS60323G.

(4) Hori, Y. Electrochemical CO2 Reduction on Metal Electrodes. In *Modern Aspects of Electrochemistry*; Vayenas, C. G., White, R. E., Gamboa-Aldeco, M. E., Eds.; Springer New York: New York, NY, 2008; Vol. 42, pp 89–189.

(5) Li, C. W.; Ciston, J.; Kanan, M. W. Electroreduction of Carbon Monoxide to Liquid Fuel on Oxide-Derived Nanocrystalline Copper. *Nature* **2014**, *508* (7497), 504–507. https://doi.org/10.1038/nature13249.

(6) Loiudice, A.; Lobaccaro, P.; Kamali, E. A.; Thao, T.; Huang, B. H.; Ager, J. W.; Buonsanti, R. Tailoring Copper Nanocrystals towards C $_2$ Products in Electrochemical CO $_2$ Reduction. *Angewandte Chemie International Edition* **2016**, *55* (19), 5789–5792. https://doi.org/10.1002/anie.201601582.
(7) Kuhl, K. P.; Hatsukade, T.; Cave, E. R.; Abram, D. N.; Kibsgaard, J.; Jaramillo, T. F. Electrocatalytic Conversion of Carbon Dioxide to Methane and Methanol on Transition Metal Surfaces. *Journal of the American Chemical Society* **2014**, *136* (40), 14107–14113. https://doi.org/10.1021/ja505791r.
(8) He, J.; Johnson, N. J. J.; Huang, A.; Berlinguette, C. P. Electrocatalytic Alloys for CO2 Reduction. *ChemSusChem* **2018**, *11* (1), 48–57. https://doi.org/10.1002/cssc.201701825.
(9) Conway, B. E. *Electrochemical Supercapacitors: Scientific Fundamentals and Technological Applications*; Springer US, 1999.
(10) Kodintsev, I. M.; Trasatti, S. Electrocatalysis of H2 Evolution on RuO2 + IrO2 Mixed Oxide Electrodes. *Electrochimica Acta* **1994**, *39* (11–12), 1803–1808. https://doi.org/10.1016/0013-4686(94)85168-9.
(11) Karlsson, R. K. B.; Cornell, A. Selectivity between Oxygen and Chlorine Evolution in the Chlor-Alkali and Chlorate Processes. *Chemical Reviews* **2016**, *116* (5), 2982–3028. https://doi.org/10.1021/acs.chemrev.5b00389.
(12) Reier, T.; Nong, H. N.; Teschner, D.; Schlögl, R.; Strasser, P. Electrocatalytic Oxygen Evolution Reaction in Acidic Environments - Reaction Mechanisms and Catalysts. *Advanced Energy Materials* **2017**, *7* (1), 1601275. https://doi.org/10.1002/aenm.201601275.
(13) Bandi, A. Electrochemical Reduction of Carbon Dioxide on Conductive Metallic Oxides. *Journal of the Electrochemical Society* **1990**, *137* (7), 2157–2160.
(14) Bandi, A.; Kühne, H.-M. Electrochemical Reduction of Carbon Dioxide in Water: Analysis of Reaction Mechanism on Ruthenium-Titanium-Oxide. *Journal of the Electrochemical Society* **1992**, *139* (6), 1605–1610.
(15) Popić, J. P.; Avramov-Ivić, M. L.; Vuković, N. B. Reduction of Carbon Dioxide on Ruthenium Oxide and Modified Ruthenium Oxide Electrodes in 0.5 M NaHCO3. *Journal of Electroanalytical Chemistry* **1997**, *421* (1–2), 105–110. https://doi.org/10.1016/S0022-0728(96)04823-1.
(16) Qu, J.; Zhang, X.; Wang, Y.; Xie, C. Electrochemical Reduction of CO2 on RuO2/TiO2 Nanotubes Composite Modified Pt Electrode. *Electrochimica Acta* **2005**, *50* (16–17), 3576–3580. https://doi.org/10.1016/j.electacta.2004.11.061.
(17) Ullah, N.; Ali, I.; Jansen, M.; Omanovic, S. Electrochemical Reduction of CO $_2$ in an Aqueous Electrolyte Employing an Iridium/Ruthenium-Oxide Electrode. *The Canadian Journal of Chemical Engineering* **2015**, *93* (1), 55–62. https://doi.org/10.1002/cjce.22110.
(18) Karamad, M.; Hansen, H. A.; Rossmeisl, J.; Nørskov, J. K. Mechanistic Pathway in the Electrochemical Reduction of CO $_2$ on RuO $_2$. *ACS Catalysis* **2015**, *5* (7), 4075–4081. https://doi.org/10.1021/cs501542n.
(19) Bhowmik, A.; Vegge, T.; Hansen, H. A. Descriptors and Thermodynamic Limitations of Electrocatalytic Carbon Dioxide Reduction on Rutile Oxide Surfaces. *ChemSusChem* **2016**, *9* (22), 3230–3243. https://doi.org/10.1002/cssc.201600845.
(20) Bhowmik, A.; Hansen, H. A.; Vegge, T. Role of CO* as a Spectator in CO $_2$ Electroreduction on RuO $_2$. *The Journal of Physical Chemistry C* **2017**, *121* (34), 18333–18343. https://doi.org/10.1021/acs.jpcc.7b04242.

(21) Bhowmik, A.; Hansen, H. A.; Vegge, T. Electrochemical Reduction of CO_2 on $Ir_xRu_{(1-x)}O_2$ (110) Surfaces. *ACS Catalysis* **2017**, *7* (12), 8502–8513. https://doi.org/10.1021/acscatal.7b02914.
(22) Over, H. Surface Chemistry of Ruthenium Dioxide in Heterogeneous Catalysis and Electrocatalysis: From Fundamental to Applied Research. *Chemical Reviews* **2012**, *112* (6), 3356–3426. https://doi.org/10.1021/cr200247n.
(23) Rao, R. R.; Kolb, M. J.; Halck, N. B.; Pedersen, A. F.; Mehta, A.; You, H.; Stoerzinger, K. A.; Feng, Z.; Hansen, H. A.; Zhou, H.; et al. Towards Identifying the Active Sites on RuO_2 (110) in Catalyzing Oxygen Evolution. *Energy & Environmental Science* **2017**, *10* (12), 2626–2637. https://doi.org/10.1039/C7EE02307C.
(24) Lee, Y.; Suntivich, J.; May, K. J.; Perry, E. E.; Shao-Horn, Y. Synthesis and Activities of Rutile IrO_2 and RuO_2 Nanoparticles for Oxygen Evolution in Acid and Alkaline Solutions. *The Journal of Physical Chemistry Letters* **2012**, *3* (3), 399–404. https://doi.org/10.1021/jz2016507.
(25) Kuhn, A. T.; Mortimer, C. J. The Kinetics of Chlorine Evolution and Reduction on Titanium-Supported Metal Oxides Especially RuO[Sub 2] and IrO[Sub 2]. *Journal of The Electrochemical Society* **1973**, *120* (2), 231. https://doi.org/10.1149/1.2403425.
(26) Aromaa, J.; Forsén, O. Evaluation of the Electrochemical Activity of a Ti–RuO2–TiO2 Permanent Anode. *Electrochimica Acta* **2006**, *51* (27), 6104–6110. https://doi.org/10.1016/j.electacta.2005.12.053.
(27) Ardizzone, S.; Falciola, M.; Trasatti, S. Effect of the Nature of the Precursor on the Electrocatalytic Properties of Thermally Prepared Ruthenium Oxide. *Journal of The Electrochemical Society* **1989**, *136* (5), 1545–1550.
(28) Sugimoto, W.; Kizaki, T.; Yokoshima, K.; Murakami, Y.; Takasu, Y. Evaluation of the Pseudocapacitance in RuO2 with a RuO2/GC Thin Film Electrode. *Electrochimica Acta* **2004**, *49* (2), 313–320. https://doi.org/10.1016/j.electacta.2003.08.013.
(29) Ardizzone, S.; Fregonara, G.; Trasatti, S. "Inner" and "Outer" Active Surface of RuO2 Electrodes. *Electrochimica Acta* **1990**, *35* (1), 263–267. https://doi.org/10.1016/0013-4686(90)85068-X.
(30) Hess, F.; Sack, C.; Langsdorf, D.; Over, H. Probing the Activity of Different Oxygen Species in the CO Oxidation over RuO_2 (110) by Combining Transient Reflection–Absorption Infrared Spectroscopy with Kinetic Monte Carlo Simulations. *ACS Catalysis* **2017**, *7* (12), 8420–8428. https://doi.org/10.1021/acscatal.7b02838.
(31) Yajima, T.; Uchida, H.; Watanabe, M. In-Situ ATR-FTIR Spectroscopic Study of Electro-Oxidation of Methanol and Adsorbed CO at Pt−Ru Alloy. *The Journal of Physical Chemistry B* **2004**, *108* (8), 2654–2659. https://doi.org/10.1021/jp037215q.
(32) Katayama, Y.; Giordano, L.; Rao, R. R.; Hwang, J.; Muroyama, H.; Matsui, T.; Eguchi, K.; Shao-Horn, Y. Surface (Electro)Chemistry of CO_2 on Pt Surface: An *in Situ* Surface-Enhanced Infrared Absorption Spectroscopy Study. *The Journal of Physical Chemistry C* **2018**, *122* (23), 12341–12349. https://doi.org/10.1021/acs.jpcc.8b03556.
(33) Gaudet, J.; Tavares, A. C.; Trasatti, S.; Guay, D. Physicochemical Characterization of Mixed RuO_2-SnO_2 Solid Solutions. *Chemistry of Materials* **2005**, *17* (6), 1570–1579. https://doi.org/10.1021/cm048129l.
(34) Wang, X.; Shao, Y.; Liu, X.; Tang, D.; Wu, B.; Tang, Z.; Wang, X.; Lin, W. Phase Stability and Phase Structure of Ru–Ti–O Complex Oxide Electrocatalyst. *Journal of the American Ceramic Society* **2015**, *98* (6), 1915–1924. https://doi.org/10.1111/jace.13398.

(35) Trasatti, S. Physical Electrochemistry of Ceramic Oxides. *Electrochimica Acta* **1991**, *36* (2), 225–241.
(36) Kameyama, K. Surface Characterization of RuO[Sub 2]-IrO[Sub 2]-TiO[Sub 2] Coated Titanium Electrodes. *Journal of The Electrochemical Society* **1994**, *141* (3), 643. https://doi.org/10.1149/1.2054784.
(37) Colomer, M. T.; Jurado, J. R. Structural, Microstructural, and Electrical Transport Properties of TiO_2 −RuO_2 Ceramic Materials Obtained by Polymeric Sol−Gel Route. *Chemistry of Materials* **2000**, *12* (4), 923–930. https://doi.org/10.1021/cm9903879.
(38) Kuhl, K. P.; Cave, E. R.; Abram, D. N.; Jaramillo, T. F. New Insights into the Electrochemical Reduction of Carbon Dioxide on Metallic Copper Surfaces. *Energy & Environmental Science* **2012**, *5* (5), 7050. https://doi.org/10.1039/c2ee21234j.
(39) Dutta, A.; Kuzume, A.; Rahaman, M.; Vesztergom, S.; Broekmann, P. Monitoring the Chemical State of Catalysts for CO_2 Electroreduction: An In Operando Study. *ACS Catalysis* **2015**, *5* (12), 7498–7502. https://doi.org/10.1021/acscatal.5b02322.
(40) Chen, Y.; Kanan, M. W. Tin Oxide Dependence of the CO_2 Reduction Efficiency on Tin Electrodes and Enhanced Activity for Tin/Tin Oxide Thin-Film Catalysts. *Journal of the American Chemical Society* **2012**, *134* (4), 1986–1989. https://doi.org/10.1021/ja2108799.
(41) Spataru, N.; Tokuhiro, K.; Terashima, C.; Rao, T. N.; Fujishima, A. Electrochemical Reduction of Carbon Dioxide at Ruthenium Dioxide Deposited on Boron-Doped Diamond. *Journal of Applied Electrochemistry* **2003**, *33* (12), 1205–1210. https://doi.org/10.1023/B:JACH.0000003866.85015.b6.
(42) Clark, E. L.; Resasco, J.; Landers, A.; Lin, J.; Chung, L.-T.; Walton, A.; Hahn, C.; Jaramillo, T. F.; Bell, A. T. Standards and Protocols for Data Acquisition and Reporting for Studies of the Electrochemical Reduction of Carbon Dioxide. *ACS Catalysis* **2018**, *8* (7), 6560–6570. https://doi.org/10.1021/acscatal.8b01340.
(43) Wuttig, A.; Surendranath, Y. Impurity Ion Complexation Enhances Carbon Dioxide Reduction Catalysis. *ACS Catalysis* **2015**, *5* (7), 4479–4484. https://doi.org/10.1021/acscatal.5b00808.
(44) Bertheussen, E.; Abghoui, Y.; Jovanov, Z. P.; Varela, A.-S.; Stephens, I. E. L.; Chorkendorff, I. Quantification of Liquid Products from the Electroreduction of CO 2 and CO Using Static Headspace-Gas Chromatography and Nuclear Magnetic Resonance Spectroscopy. *Catalysis Today* **2017**, *288*, 54–62. https://doi.org/10.1016/j.cattod.2017.02.029.
(45) Wang, W. B.; Zei, M. S.; Ertl, G. Electrooxidation of CO on Ru(0001) and RuO2(100) Electrode Surfaces. *Chemical Physics Letters* **2002**, *355* (3–4), 301–305. https://doi.org/10.1016/S0009-2614(02)00263-4.
(46) Lin, W. F.; Jin, J. M.; Christensen, P. A.; Scott, K. Structure and Reactivity of the Ru(0001) Electrode towards Fuel Cell Electrocatalysis. *Electrochimica Acta* **2003**, *48* (25–26), 3815–3822. https://doi.org/10.1016/S0013-4686(03)00515-2.
(47) Yamakata, A.; Osawa, M. Destruction of the Water Layer on a Hydrophobic Surface Induced by the Forced Approach of Hydrophilic and Hydrophobic Cations. *The Journal of Physical Chemistry Letters* **2010**, *1* (9), 1487–1491. https://doi.org/10.1021/jz100424e.
(48) Ktz, E. R.; Stucki, S. Ruthenium Dioxide as a Hydrogen-Evolving Cathode. *Journal of Applied Electrochemistry* **1987**, *17* (6), 1190–1197. https://doi.org/10.1007/BF01023602.

(49) Chabanier, C.; Guay, D. Activation and Hydrogen Absorption in Thermally Prepared RuO2 and IrO2. *Journal of Electroanalytical Chemistry* **2004**, *570* (1), 13–27. https://doi.org/10.1016/j.jelechem.2004.03.014.
(50) Burke, L. D.; Naser, N. S. Metastability and Electrocatalytic Activity of Ruthenium Dioxide Cathodes Used in Water Electrolysis Cells. *Journal of Applied Electrochemistry* **2005**, *35* (9), 931–938. https://doi.org/10.1007/s10800-005-5290-8.
(51) Weber, T.; Abb, M.; Khalid, O.; Pfrommer, J.; Carla, F.; Znaiguia, R.; Vonk, V.; Stierle, A.; Over, H. In-Situ Studies of the Electrochemical Reduction of Supported Ultrathin Single Crystalline RuO_2 (110) Layer in Acidic Environment. *The Journal of Physical Chemistry C* **2019**. https://doi.org/10.1021/acs.jpcc.8b10741.
(52) Blouin, M.; Guay, D. Activation of Ruthenium Oxide, Iridium Oxide, and Mixed RuxIr1- x Oxide Electrodes during Cathodic Polarization and Hydrogen Evolution. *Journal of the electrochemical society* **1997**, *144* (2), 573–581.
(53) Karlsson, R. K. B.; Cornell, A.; Pettersson, L. G. M. Structural Changes in RuO_2 during Electrochemical Hydrogen Evolution. *The Journal of Physical Chemistry C* **2016**, *120* (13), 7094–7102. https://doi.org/10.1021/acs.jpcc.5b11696.
(54) Juodkazytė, J.; Vilkauskaitė, R.; Šebeka, B.; Juodkazis, K. Difference between Surface Electrochemistry of Ruthenium and RuO_2 Electrodes. *Transactions of the IMF* **2007**, *85* (4), 194–201. https://doi.org/10.1179/174591907X16413.
(55) Chen, L.; Guay, D.; Lasia, A. Kinetics of the Hydrogen Evolution Reaction on RuO2 and IrO2 Oxide Electrodes in H 2 SO 4 Solution: An AC Impedance Study. *Journal of The Electrochemical Society* **1996**, *143* (11), 3576–3584.
(56) Pastor, E.; Le Formal, F.; Mayer, M. T.; Tilley, S. D.; Francàs, L.; Mesa, C. A.; Grätzel, M.; Durrant, J. R. Spectroelectrochemical Analysis of the Mechanism of (Photo)Electrochemical Hydrogen Evolution at a Catalytic Interface. *Nature Communications* **2017**, *8*, 14280. https://doi.org/10.1038/ncomms14280.
(57) Zhang, Y.-J.; Sethuraman, V.; Michalsky, R.; Peterson, A. A. Competition between CO_2 Reduction and H_2 Evolution on Transition-Metal Electrocatalysts. *ACS Catalysis* **2014**, *4* (10), 3742–3748. https://doi.org/10.1021/cs5012298.
(58) Varela, A. S.; Schlaup, C.; Jovanov, Z. P.; Malacrida, P.; Horch, S.; Stephens, I. E. L.; Chorkendorff, I. CO_2 Electroreduction on Well-Defined Bimetallic Surfaces: Cu Overlayers on Pt(111) and Pt(211). *The Journal of Physical Chemistry C* **2013**, *117* (40), 20500–20508. https://doi.org/10.1021/jp406913f.
(59) Hoshi, N.; Suzuki, T.; Hori, Y. Step Density Dependence of Co2 Reduction Rate on Pt(S)-[n(111) × (111)] Single Crystal Electrodes. *Electrochimica Acta* **1996**, *41* (10), 1647–1653. https://doi.org/10.1016/0013-4686(95)00418-1.
(60) Taguchi, S.; Aramata, A.; Enyo, M. Reduced CO2 on Polycrystalline Pd and Pt Electrodes in Neutral Solution: Electrochemical and in Situ Fourier Transform IR Studies. *Journal of Electroanalytical Chemistry* **1994**, *372* (1–2), 161–169. https://doi.org/10.1016/0022-0728(93)03287-Y.
(61) Miki, A.; Ye, S.; Osawa, M. Surface-Enhanced IR Absorption on Platinum Nanoparticles: An Application to Real-Time Monitoring of Electrocatalytic Reactions. *Chemical Communications* **2002**, No. 14, 1500–1501. https://doi.org/10.1039/b203392e.
(62) Osawa, M.; Yoshii, K.; Ataka, K.; Yotsuyanagi, T. Real-Time Monitoring of Electrochemical Dynamics by Submillisecond Time-Resolved Surface-Enhanced Infrared

Attenuated-Total-Reflection Spectroscopy. *Langmuir* **1994**, *10* (3), 640–642. https://doi.org/10.1021/la00015a009.

(63) Chen, Y. X.; Miki, A.; Ye, S.; Sakai, H.; Osawa, M. Formate, an Active Intermediate for Direct Oxidation of Methanol on Pt Electrode. *Journal of the American Chemical Society* **2003**, *125* (13), 3680–3681. https://doi.org/10.1021/ja029044t.

TOC

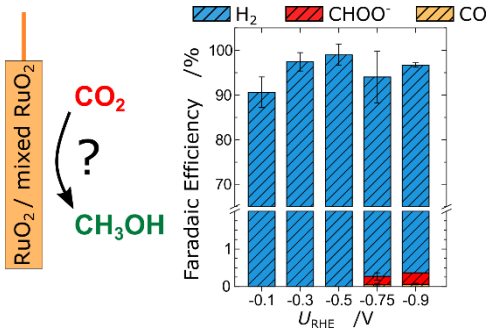
RuO2/ mixed RuO2
CO2
?
CH3OH
H2
CHOO-
CO
Faradaic Efficiency /%
100
90
80
70
1
0
-0.1
-0.3
-0.5
-0.75
-0.9
URHE /V